Numerical Analysis of Pulse Broadening in Graded Index Optical Fibers

KATSUMI MORISHITA, MEMBER, IEEE

Abstract—**A scalar multilayer approximation method for calculating the impulse response of multimode optical fibers from measured refractive-index profiles is described. A comparison is made between shapes of measured pulses and calculated pulses.**

I. Introduction

MUCH EFFORT has been expended on designing multimode optical fibers that will have sufficient information-carrying capacity. However, manufactured fibers have various impulse responses and bandwidths because of departures of the index profile from its optimum shape. If the group velocity and attenuation of each propagation mode are calculated from measured refractive-index profiles, the impulse responses and fiber bandwidths can be predicted. Furthermore, on the basis of the knowledge of the group velocity and attenuation, we can splice actual fibers to reduce the pulse broadening in the spliced fibers.

It is the purpose of this paper to describe a method for calculating the impulse responses of multimode optical fibers from measured refractive-index profiles. For this purpose, Marcuse [1] proposed a computational method which is based on the WKB theory and Okamoto [2] presented a method using the finite element analysis. In the present paper, a practical method using the scalar multilayer approximation and the integral expression for the group velocity [3] is described. The group velocity and attenuation of every mode are computed by this method, and impulse responses are predicted. The calculated impulse responses are compared with the measured ones for on-axis and off-axis excitations. The good agreement found between theory and experiment demonstrates an ability to predict pulse broadening in fibers having general index profiles.

II. Scalar Multilayer Approximation Analysis

Since exact analysis for graded index optical fibers is difficult and time-consuming, appropriate approximation techniques have been developed. Among them, scalar approximation analysis is one of the most widely used techniques. The accuracy of scalar approximation technique in optical fiber analysis was investigated in detail [4], [5]. The error due to the scalar approximation is thought to be sufficiently small for calculating impulse responses in multimode optical fibers.

Manuscript received September 12, 1980; revised December 2, 1980.

The author is with the Department of Electrical Communication Engineering, Osaka University, Osaka, 565 Japan.

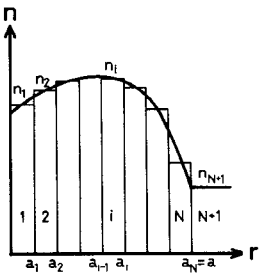

Fig. 1. Multilayer approximation of the refractive-index profile. The core radius is a.

It is assumed that the permittivity ϵ of the fiber depends only upon the distance r from the axis, and the permeability is equal to that of vacuum μ_0. Applying the scalar approximation conditions into Maxwell's equations, we get the following scalar wave equation:

$$\frac{d^2\phi}{dr^2}+\frac{1}{r}\frac{d\phi}{dr}+\left(\omega^2\epsilon(r)\mu_0-\beta^2-\frac{m^2}{r^2}\right)\phi=0 \qquad (1)$$

where β is a propagation constant of the guided mode, transverse Cartesian components of the electromagnetic fields, i.e., E_x, E_y, H_x, and H_y, are expressed as

$$\left.\begin{matrix}E_x, & E_y\\ H_x, & H_y\end{matrix}\right\}=\phi(r)\left\{\begin{matrix}\sin m\theta\\ \cos m\theta\end{matrix}\right\}. \qquad (2)$$

The refractive-index profile in the core region is represented approximately by a stratified multilayer structure, as shown in Fig. 1. The scalar wave equation in the ith layer can be expressed as

$$\frac{d^2\phi}{dr^2}+\frac{1}{r}\frac{d\phi}{dr}+\left(k^2n_i^2-\beta^2-\frac{m^2}{r^2}\right)\phi=0 \qquad (3)$$

where $k=\omega\sqrt{\epsilon_0\mu_0}$, and n_i represents the refractive-index of the ith layer. The foregoing equation is solved exactly, and the propagation constant β and the field distribution ϕ are determined so that ϕ and $d\phi/dr$ are continuous across the discontinuity boundary $r=a_i$.

The solutions of (3) are represented by Bessel functions, and ϕ and $d\phi/dr$ in the ith layer $(a_{i-1}<r\leq a_i)$ are expressed as

$$\begin{bmatrix}\phi\\ \frac{1}{\beta}\frac{d\phi}{dr}\end{bmatrix}=\begin{bmatrix}Z_m(u_ir) & \bar{Z}_m(u_ir)\\ \frac{u_i}{\beta}Z'_m(u_ir) & \frac{u_i}{\beta}\bar{Z}'_m(u_ir)\end{bmatrix}\begin{bmatrix}A_i\\ B_i\end{bmatrix} \qquad (4)$$

where A_i and B_i are unknown coefficients, Z_m and $\bar{Z}_m$ are

0018-9480/81/0400-0348$00.75 ©1981 IEEE

signified as follows:

i) $Z_m(u_i r)=J_m(u_i r)$, $\bar{Z}_m(u_i r)=N_m(u_i r)$, for $u_i^2=k^2n_i^2-\beta^2>0$.

ii) $Z_m(u_i r)=I_m(u_i r)$, $\bar{Z}_m(u_i r)=K_m(u_i r)$, for $-u_i^2=k^2n_i^2-\beta^2<0$.

Let us now derive the relation between unknown coefficients (A_i, B_i) and (A_{i-1}, B_{i-1}). In the $i-1$th layer $(a_{i-2}<r\leqslant a_{i-1})$, ϕ and $d\phi/dr$ are written as

$$\begin{bmatrix} \phi \\ \frac{1}{\beta}\frac{d\phi}{dr} \end{bmatrix}=\begin{bmatrix} Z_m(u_{i-1}r) & \bar{Z}_m(u_{i-1}r) \\ \frac{u_{i-1}}{\beta}Z'_m(u_{i-1}r) & \frac{u_{i-1}}{\beta}\bar{Z}'_m(u_{i-1}r) \end{bmatrix}\begin{bmatrix} A_{i-1} \\ B_{i-1} \end{bmatrix}. \tag{5}$$

Using that ϕ and $d\phi/dr$ are continuous across the discontinuity boundary $r=a_{i-1}$, we can get the following equation:

$$\begin{bmatrix} Z_m(u_i a_{i-1}) & \bar{Z}_m(u_i a_{i-1}) \\ \frac{u_i}{\beta}Z'_m(u_i a_{i-1}) & \frac{u_i}{\beta}\bar{Z}'_m(u_i a_{i-1}) \end{bmatrix}\begin{bmatrix} A_i \\ B_i \end{bmatrix}$$

$$=\begin{bmatrix} Z_m(u_{i-1}a_{i-1}) & \bar{Z}_m(u_{i-1}a_{i-1}) \\ \frac{u_{i-1}}{\beta}Z'_m(u_{i-1}a_{i-1}) & \frac{u_{i-1}}{\beta}\bar{Z}'_m(u_{i-1}a_{i-1}) \end{bmatrix}\begin{bmatrix} A_{i-1} \\ B_{i-1} \end{bmatrix}. \tag{6}$$

The relation between (A_i, B_i) and (A_{i-1}, B_{i-1}) is derived from (6) as follows:

$$\begin{bmatrix} A_i \\ B_i \end{bmatrix}=\boldsymbol{P}_{i-1}\begin{bmatrix} A_{i-1} \\ B_{i-1} \end{bmatrix} \tag{7}$$

where

$$\boldsymbol{P}_{i-1}=\begin{bmatrix} Z_m(u_i a_{i-1}) & \bar{Z}_m(u_i a_{i-1}) \\ \frac{u_i}{\beta}Z'_m(u_i a_{i-1}) & \frac{u_i}{\beta}\bar{Z}'_m(u_i a_{i-1}) \end{bmatrix}^{-1}$$

$$\times\begin{bmatrix} Z_m(u_{i-1}a_{i-1}) & \bar{Z}_m(u_{i-1}a_{i-1}) \\ \frac{u_{i-1}}{\beta}Z'_m(u_{i-1}a_{i-1}) & \frac{u_{i-1}}{\beta}\bar{Z}'_m(u_{i-1}a_{i-1}) \end{bmatrix}. \tag{8}$$

By using (7), the unknown coefficients in the ith layer (A_i, B_i) can be expressed in terms of the coefficients in the first layer (A_1, B_1) as follows:

$$\begin{bmatrix} A_i \\ B_i \end{bmatrix}=\boldsymbol{P}_{i-1}\boldsymbol{P}_{i-2}\cdots\boldsymbol{P}_1\begin{bmatrix} A_1 \\ B_1 \end{bmatrix}. \tag{9}$$

Since the electromagnetic field ϕ is finite at $r=0$ and ∞, the coefficients B_1, A_{N+1} must satisfy

$$B_1=0 \quad A_{N+1}=0. \tag{10}$$

The relation between coefficients in the first layer and the cladding (the $N+1$th layer) is derived from (9) and (10) as follows:

$$\begin{bmatrix} 0 \\ B_{N+1} \end{bmatrix}=\boldsymbol{P}\begin{bmatrix} A_1 \\ 0 \end{bmatrix} \tag{11}$$

where

$$\boldsymbol{P}=\begin{bmatrix} P_{11} & P_{12} \\ P_{21} & P_{22} \end{bmatrix}=\boldsymbol{P}_N\boldsymbol{P}_{N-1}\cdots\boldsymbol{P}_1. \tag{12}$$

In order that nontrivial solutions of (11) exist

$$P_{11}=0 \tag{13}$$

must be satisfied. The propagation constants can be determined by the eigenvalue equation (13), and the coefficients (A_i, B_i) can be obtained from (9).

The group velocity V_g obtained by the scalar approximation method is expressed as [3]

$$\frac{V_g}{C}=\frac{\beta}{k}\frac{\int_0^\infty \phi^2 r\,dr}{\int_0^\infty n\frac{d(kn)}{dk}\phi^2 r\,dr} \tag{14}$$

where C is the velocity of light in vacuum. The refractive-index in multilayer approximation analysis is constant in each layer. Therefore, the expression for the group velocity, (14), can be rewritten in the form

$$\frac{V_g}{C}=\frac{\beta}{k}\frac{\sum_i I_i}{\sum_i\left(n_i^2-n_i\lambda\frac{dn_i}{d\lambda}\right)I_i} \tag{15}$$

where

$$I_i=\int_{a_{i-1}}^{a_i}\left\{A_i Z_m(u_i r)+B_i\bar{Z}_m(u_i r)\right\}^2 r\,dr.$$

Since the integration I_i can be analytically obtained as shown in the Appendix and the coefficients (A_i, B_i) are given by (9), the group velocity V_g is determined by using (15) without numerical integration.

Assuming that all guided modes propagate independently from each other and suffer only the attenuation due to bulk loss from absorption and Rayleigh scattering, the attenuation constant α_M of the propagation mode M is approximately represented as

$$\alpha_M=\sum_i\frac{P_{Mi}}{P_M}\alpha_i \tag{16}$$

where P_{Mi} expresses the power fraction in the ith layer of mode M, P_M is the total power of mode M, i.e., $P_M=\Sigma_i P_{Mi}$, and α_i is the bulk loss in the ith layer. Using (15) and (16), the power of mode M at propagation distance L, $P_M(L)$, the delay time per fiber length L of mode M, τ_M, the average delay time per fiber length L, $\bar{\tau}$, and the rms pulsewidth, σ, are given by

$$P_M(L)=P_{0M}e^{-\alpha_M L} \tag{17}$$

$$\tau_M=\frac{L}{V_{gM}} \tag{18}$$

$$\bar{\tau}=\frac{\sum_M\{\tau_M P_M(L)\}}{\sum_M P_M(L)} \tag{19}$$

$$\sigma^2=\frac{1}{\sum_M P_M(L)}\sum_M\left\{P_M(L)(\tau_M-\bar{\tau})^2\right\} \tag{20}$$

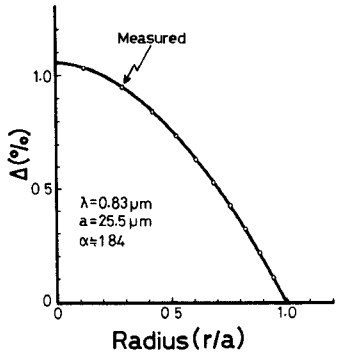

Fig. 2. Refractive-index profile from [6].

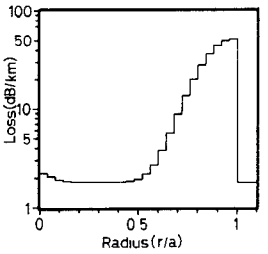

Fig. 3. Bulk loss distribution as a function of radius r.

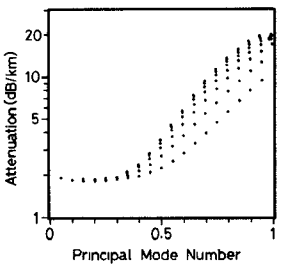

Fig. 4. Differential mode attenuation as a function of the normalized principal mode number.

where P_{0M} and V_{gM} are the incident power and the group velocity of mode M, respectively.

III. Numerical Results

The shape of the impulse response, the total loss, and the rms pulsewidth are computed from the refractive-index profile shown in Fig. 2, and are compared with the measured results. The coupling length of the fiber with the profile shown in Fig. 2 is several tens of kilometers [6]. Since the propagation distance ($L=1048$ m) of pulses in this measurements is much shorter than the coupling length, mode coupling is assumed to be negligible.

In this numerical analysis, the refractive-index profile is divided into 25 layers. Assuming that the bulk loss of each layer is shown in Fig. 3, the differential mode attenuation, which is similar to the typical measurement results [7], is computed, as shown in Fig. 4. Since the fiber is fabricated by modified chemical vapor deposition of GeO_2-doped fused silica, it is considered that the absorption loss is small and about the same in core and cladding. Hence, it is presumable that the Rayleigh scattering approximately increases with the distance from the axis in the core and is a little greater on the vicinity of the axis because of the index fluctuations caused by the collapsing process.

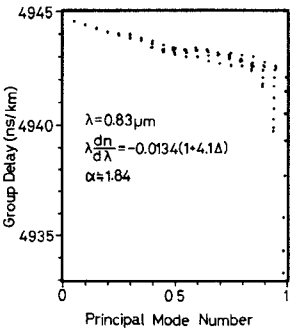

Fig. 5. Group delay as a function of the normalized principal mode number.

Material dispersion of GeO_2-doped fused silica is approximately expressed as

$$\lambda\frac{dn}{d\lambda}=\lambda\frac{dn_2}{d\lambda}\left\{1+\Delta\left(1+\frac{n_2}{\lambda\frac{dn_2}{d\lambda}}P\right)\right\} \tag{21}$$

where n_2 is the refractive-index of pure silica, Δ is the refractive-index difference, and P is given by

$$P=\frac{\lambda}{\Delta}\frac{d\Delta}{d\lambda}. \tag{22}$$

From the measurement results of Malitson [8] and Presby *et al.* [9], (21) is given at $\lambda=0.83$ μm as follows:

$$\lambda\frac{dn}{d\lambda}=-0.0134(1+4.1\Delta). \tag{23}$$

The group delay of each propagation mode is computed by using (23) and Fig. 2, and is shown in Fig. 5. Since the group delay approximately decreases with the principal mode number, the index profile shown in Fig. 2 turns out not to be optimum. To obtain the optimum power-law refractive-index fiber made of GeO_2-doped fused silica, the exponent of power-law profile must be made larger than the exponent ($\alpha\simeq 1.84$) of the fiber shown in Fig. 2. For the practical use of the fiber shown in Fig. 2, it had better be spliced with the fiber in which the group delay increases with the principal mode number in order to equalize group delay differences.

The calculated and experimental impulse responses are compared. Fig. 6 shows the impulse responses measured with a semiconductor pulse laser at $\lambda=0.83$ μm. The input pulse is shown in Fig. 6(a). Output pulses for on-axis and off-axis excitations are shown in Fig. 6(b) and Fig. 6(c), respectively. Assuming that Fig. 7 shows input modal power distributions for on-axis and off-axis excitations, output pulses at propagation distance $L=1048$ m are computed as shown in Fig. 8. The calculated pulsewidth and pulse shape for each excitation show good agreement with the measurement results. The calculated pulsewidths are a little narrower than the measured ones because of ignoring broadening of the pulse carried by each mode.

Computing the rms pulsewidth and the pulse shape requires approximately 11 min of running time on the

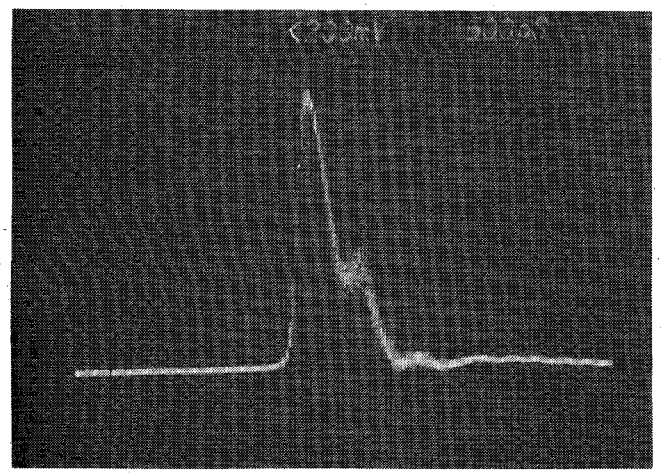

(a)

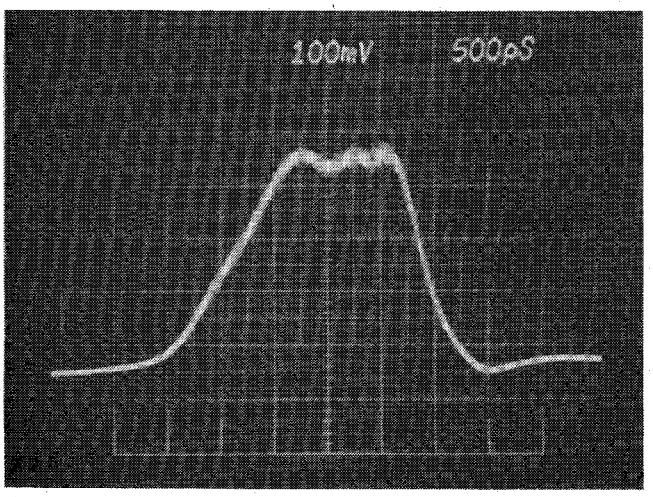

(b)

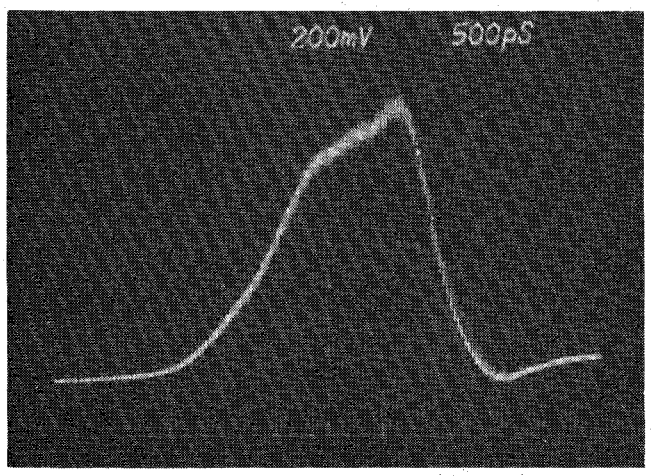

(c)

Fig. 6. Input and output pulses from [6]. Vertical scale is arbitrary. Time scale is 500 ps/div. (a) Input pulse. (b) Output pulse for on-axis excitation. (c) Output pulse for off-axis excitation.

ACOS-900(NEC) computer for the measured fiber which has about 400 propagation modes. In this analysis, when refractive-index profiles are divided into N layers, it takes N times the computer time for the calculation of each eigenvalue.

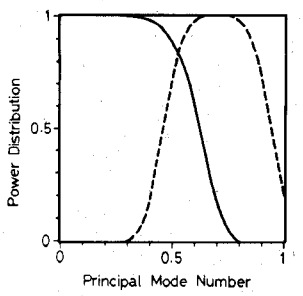

Fig. 7. Input modal power distribution. _____ on-axis excitation; -------- off-axis excitation.

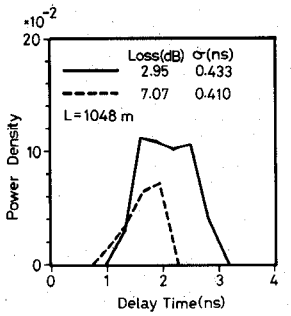

Fig. 8. Calculated output pulse. _____ on-axis excitation; -------- off-axis excitation.

IV. Conclusions

A method for calculating the impulse responses of multimode optical fibers from measured refractive-index profiles is described. A comparison is made between shapes of measured pulses and calculated pulses. This method that includes the effect of dispersive properties of core and cladding glasses and the modal power distribution has given good predictions of the output pulse shape. It has become evident that this computation method is one of the most practical methods to predict fiber bandwidth from measured refractive-index profiles.

Appendix

$$\int Z_m(ur)^2 r\,dr = \frac{r^2}{2}\left\{Z_m(ur)^2 - Z_{m-1}(ur)Z_{m+1}(ur)\right\} \tag{A1}$$

where $Z_m(ur)$ expresses $J_m(ur)$, $N_m(ur)$, $I_m(ur)$, or $K_m(ur)$.

$$\int J_m(ur)N_m(ur)r\,dr = \frac{r^2}{4}\left\{2J_m(ur)N_m(ur) - J_{m-1}(ur)N_{m+1}(ur) - J_{m+1}(ur)N_{m-1}(ur)\right\} \tag{A2}$$

$$\int I_m(ur)K_m(ur)r\,dr = \frac{r^2}{4}\left\{2I_m(ur)K_m(ur) + I_{m-1}(ur)K_{m+1}(ur) + I_{m+1}(ur)K_{m-1}(ur)\right\}. \tag{A3}$$

ACKNOWLEDGMENT

The author wishes to thank Prof. N. Kumagai of Osaka University for his encouragement and K. Kitayama of Nippon Telegraph and Telephone Public Corporation for providing the experimental data and valuable discussions.

REFERENCES

[1] D. Marcuse, "Calculation of bandwidth from index profiles of optical fibers. 1: Theory," *J. Appl. Opt.*, vol. 18, no. 12, p. 2073, June 1979.
[2] K. Okamoto, "Comparison of calculated and measured impulse responses of optical fibers," *J. Appl. Opt.*, vol. 18, no. 13, p. 2199, July 1979.
[3] K. M. Case, "On wave propagation in inhomogenious media," *J. Math. Phys.*, vol 13, no. 3, p. 360, Mar. 1972.
[4] K. Morishita, Y. Kondoh, and N. Kumagai, "On the accuracy of scalar approximation technique in optical fiber analysis," *IEEE Trans. Microwave Theory Tech.*, vol. MTT-28, p. 33, Jan. 1980.
[5] K. Morishita, Y. Obata, and N. Kumagai, "Accuracy of the group velocity of the step-index fiber modes evaluated by the scalar approximation technique," *Trans. Inst. Electron. Commun. Eng. Japan*, vol. 64-B, no. 1, p 87, Jan. 1981.
[6] K. Kitayama, private communication.
[7] K. Kitayama, M. Tateda, S. Seikai, and N. Uchida, "Determination of mode power distribution in a parabolic-index optical fibers: Theory and application," *IEEE J. Quantum Electron.*, vol. QE-15, p. 1161, Oct. 1979.
[8] I. H. Malitson, "Interspecimen comparison of the refractive index of fused silica," *J. Opt. Soc. Amer.*, vol. 55, no. 10, p. 1205, Oct. 1965.
[9] H. M. Presby and I. P. Kaminow, "Binary silica optical fibers: refractive index and profile dispersion measurements," *J. Appl. Opt.*, vol. 15, no. 12, p. 3029, Dec. 1979.

Characteristics of Unilateral Fin-Line Structures with Arbitrarily Located Slots

L. P. SCHMIDT, TATSUO ITOH, SENIOR MEMBER, IEEE, AND HOLGER HOFMANN

Abstract— **Generalized unilateral fin-line configurations for extended millimeter-wave applications are analyzed using the equivalent transmission-line concept in the spectral domain. Numerical results for the frequency-dependent propagation constants and characteristic impedances of various structures are presented.**

I. INTRODUCTION

FIN-LINE STRUCTURES have proved to be a useful tool for the development of integrated millimeter-wave components (e.g., [1]). Conventional fin-line structures proposed to date are the unilateral, bilateral, and the antipodal fin-line [2], all of which are symmetric with respect to the *E*-plane of the shielding waveguide.

In order to improve the flexibility of this class of waveguiding structures and, thus, extending the range of application and increasing the possible degree of integration, this paper analyzes more general types of unilateral fin-lines with up to three slots in symmetric as well as asymmetric positions (Fig. 1(a)).

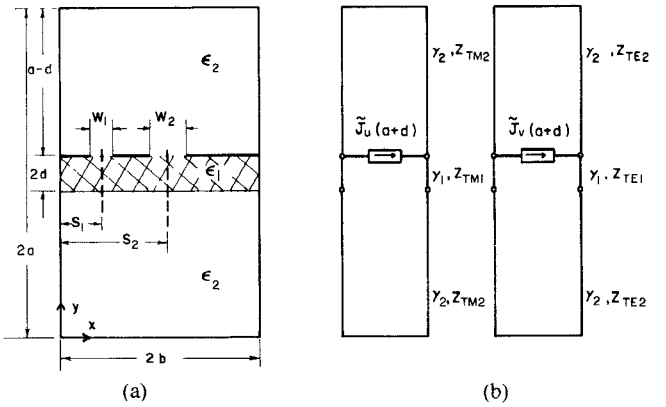

Fig. 1. Generalized unilateral fin-line (a) cross section, (b) equivalent transmission lines for TM-to-*y* and TE-to-*y* waves

This analysis includes the solution of the eigenvalue problem yielding the frequency-dependent propagation constants as well as the calculation of carefully defined characteristic impedances. Numerical results will show the improved flexibility that can be achieved by making use of this extended class of fin-line structures.

Manuscript received May 14, 1980; revised December 1, 1980. This work was supported in part by the Army Research Office under Grant DAAG29-78-G-0145. A condensed version of this paper was presented at the 1980 IEEE-MTT-S International Microwave Symposium.

L. P. Schmidt was with the Department of Electrical Engineering, The University of Texas, Austin. He is now with AEG-Telefunken, Hochfrequenztechnik, D-7900, Ulm, West Germany.
T. Itoh is with the Department of Electrical Engineering, The University of Texas, Austin.
H. Hofmann is with AEG-Telefunken, Flensburg, West Germany.

0018-9480/81/0400-0352$00.75 ©1981 IEEE